CrossMark

ORIGINAL

Distribution of the equilibrium moisture content in four hardwoods below fiber saturation point with magnetic resonance microimaging

Leandro Passarini[1] · **Cédric Malveau**[2] ·
Roger E. Hernández[1]

Abstract The distribution of liquid and bound water in wood samples under equilibrium moisture contents (EMC) below fiber saturation point (FSP) was assessed by magnetic resonance (MR) microimaging. Two Amazonian hardwoods, huayruro (*Robinia coccinea*) and cachimbo [*Cariniana domesticata*], a plantation grown eucalyptus (*Eucalyptus saligna*), and a temperate species red oak (*Quercus rubra*) were studied. Desorption tests were performed at 21 °C from full saturation state for huayruro, cachimbo, and red oak, and from green condition for eucalyptus. The EMC was reached under three desorption conditions [58, 76, and 90 % relative humidity (RH)]. MR microimages were obtained based on T_2 times and on ^{1}H concentration. Scanning electron microscopy images helped us to interpret MR microimages. The results showed that wood structure plays a major role in liquid water drainage and in water diffusion. *Eucalyptus saligna* and red oak showed liquid water entrapped in parenchyma tissues, even below FSP (90 % RH). At this same RH level, all liquid water was, however, drained for cachimbo and huayruro. For these woods, bound water was not uniformly distributed in wood structure, concentrating it more in fibers for both species. Huayruro showed the highest heterogeneity in hygroscopicity, which is explained by its particular wood anatomy.

✉ Roger E. Hernández
roger.hernandez@sbf.ulaval.ca

1 Département des sciences du bois et de la forêt, Centre de recherche sur les matériaux renouvelables, Université Laval, 2425, rue de la Terrasse, Quebec, QC G1V 0A6, Canada

2 Laboratoire de RMN, Département de chimie, Université de Montréal, 2900, boul. Édouard-Montpetit, Montreal, QC H3T 1J4, Canada

🖄 Springer

Introduction

Wood is a natural fiber composite material formed as a product of the metabolism of the living tree which, in turn, is affected by external factors such as wind, soil, and luminosity. Structural and chemical variability of wood is reflected in its physical properties such as permeability, capillary behavior, thermal conductivity, and the diffusion of bound water (Siau 1984; Panshin and de Zeeuw 1980).

One of more remarkable characteristics of wood is its hygroscopicity. Water may be present in wood in three states. Liquid water or capillary water is held in the micropores of cell walls, in the lumens of cells, and in the intercellular spaces. This water is subjected to the action of capillary pressure and thus differs from the ordinary liquid water. Bound or hygroscopic water is adsorbed by free sorption sites or by hydroxyl groups. These groups are present mainly in the macromolecules of hemicellulose and amorphous cellulose and, to a lesser extent, associated with lignin and with the surface of crystalline parts of the cellulose. Water may also be present as vapor in the lumens and in the micropores of cell walls (Stamm 1964; Navi and Heger 2005).

Moisture content has a significant effect on almost all the physical properties of wood. As the bound water content increases, wood swells, mechanical strength decreases, thermal and electrical conductivities increase, and the rate of bound water diffusion increases (Siau 1984). Bound water is sorbed at or near the sorption sites distributed throughout the surface area of the cell walls. The strong attractive forces are mainly attributed to the attraction of polar hydroxyl groups for the polar water molecules through hydrogen bonding (Skaar 1988).

Wood exchanges water molecules with the surrounding environment until reaching a dynamic equilibrium, known as equilibrium moisture content (EMC) (Skaar 1988). Relative humidity (RH) plays an important role in EMC of wood, but other factors such as temperature, sorption state (adsorption or desorption), mechanical stress, species, density, and extractable compounds may also be implied (Siau 1995).

The FSP is a very useful concept for understanding the influence of bound water on the physical and mechanical properties of wood. It was initially introduced by Tiemann (1906) as the moisture content at which the cell walls are saturated with bound water, while the lumens are free of liquid water. In other words, the FSP is a transition point between bound and liquid water (Stamm 1971). Below this point, these properties are affected by changes in the moisture content (Skaar 1988; Siau 1995). Since 1906, several studies on this concept have been advanced (Barkas 1935; Stone and Scallan 1967; Menon et al. 1987; Skaar 1988; Babiak and Kúdela 1995; Siau 1995; Hernández 2007a; Hoffmeyer et al. 2011).

However, liquid water may still be entrapped in the wood even below FSP (Hart et al. 1974; Menon et al. 1987; Araujo et al. 1992; Hernández and Bizoň 1994; Hernández and Pontin 2006; Almeida and Hernández 2006a, b; Hernández and Cáceres 2010; Passarini et al. 2014). This water could be entrapped in the less permeable flow paths in hardwoods. For sugar maple wood, liquid water appeared to

be entrapped principally in the lumina of the least accessible libriform fibers (Hernández and Cáceres 2010).

Nondestructive evaluation of wood allows studying wood properties, performance, and condition of the material without changing its end-use capabilities (Ross et al. 1998; Bucur 2003). Nuclear magnetic resonance (NMR) can provide detailed information of wood both at the microscopic and macroscopic levels, especially in the study of wood–water relations. This tool permits to study the distribution and the various states of water in wood (Araujo et al. 1992, 1993; Almeida et al. 2007; Passarini et al. 2014) from changes in the magnetization of the nuclei hydrogen in the material. In this technique, a phase of excitation is followed by a relaxation of the protons (^1H) to a lower energy state, through the phenomena of longitudinal (T_1) and transverse (T_2) relaxations (Kastler 2011).

However, the T_1 and T_2 relaxations of the water in wood are very different from that of pure water. The decay of the magnetization of the nuclei in pure water is characterized by a single exponential decay with a time constant of the order of a few seconds. Conversely, for water in a biological system, as water in wood cells, this relaxation shows a multi-exponential phenomenon produced in milliseconds or tens of milliseconds (Brownstein 1980). This behavior is a consequence of the size and shape of the cells (Brownstein and Tarr 1979). The NRM signal from green wood may be distinguished into three main components from different T_2 values: solid wood, bound water, and liquid water (Araujo et al. 1993). In this manner, the solid wood signal disappears in tens of microseconds, allowing an easy way to separate it from the cell-water signal, whose T_2 values range from one to a few milliseconds. The third component, the liquid water located in cell lumina, is characterized by T_2 values in the order of tens to hundreds of milliseconds (Hsi et al. 1977; Menon et al. 1987; Araujo et al. 1992, 1993; Thygesen and Elder 2008).

Almeida et al. (2007) used the NMR technique to separate the components of water in wood of two temperate and one tropical species at different EMCs. Three water components were observed from T_2 relaxation times analyses: slow T_2 (liquid water located in vessel elements), medium T_2 (liquid water located in fiber and parenchyma tissues), and fast T_2 (associated with bound or cell wall water). Their results also showed that, even at equilibrated conditions, during a certain range of moisture content, cell walls lost bound water even in the presence of liquid water. This range of moisture content varied according to each species. Therefore, they found liquid water at an EMC below FSP contradicting this concept.

Similar results were reported by Passarini et al. (2014) studying water state of four hardwood species below FSP with NMR technique. Besides the loss of bound water before the complete drainage of liquid water, these authors could hypothesize, from the variation observed in fast T_2 times, how water molecules were distributed and arranged in sorption sites of wood.

To have a more in depth insight into water state and EMC distribution in hardwood structure, Hernández and Cáceres (2010) used the MR microimaging technique to visualize the distribution of liquid water in sugar maple wood samples at different EMCs below FSP. The MR imaging technique has been proven effective in studying moisture content distribution in wood (Quick et al. 1990; Meder et al. 2003; Hameury and Sterley 2006; Almeida et al. 2008; Dvinskikh et al. 2011;

Telkki 2012). As the moisture content, that is ^{1}H concentration, decreases, the signal intensity will be lower. High resolution images confirmed visually the coexistence of liquid and bound water below FSP (Hernández and Cáceres 2010), a fact that has already been indirectly deduced in previous studies (Hart 1984; Menon et al. 1987; Araujo et al. 1992; Hernández and Bizoň 1994; Hernández and Pontin 2006; Almeida and Hernández 2006a, b). The drainage of all liquid water in sugar maple wood was accomplished between 76 and 86 % of RH, that is between 21.8 and 17.1 % of EMC (Hernández and Cáceres 2010), below the 30 % EMC established as FSP for this species (Hernández 2007a). SEM images obtained from the same section used for MR microimaging analysis showed that liquid water could be entrapped in the ends of the lumens of libriform fibers, or even in the intercellular spaces associated with these elements (Hernández and Cáceres 2010). Thus, it is expected that the location of the entrapped water will vary according to the wood species.

The main objective of this work was to use the MR microimaging technique to visualize liquid and bound water distribution in wood samples under EMC below FSP for four hardwood species with heterogeneous wood anatomy.

Materials and methods

Two hardwood species from Peru, namely huayruro (*Robinia coccinea* Aublet) and cachimbo [*Cariniana domestica* (C. Martius) Miers], a plantation grown eucalyptus species (*E. saligna* Smith) from Brazil, and a temperate species red oak (*Quercus rubra* L.) were used for this study. These species show a large diversity in terms of anatomical properties of wood.

Two boards of each tropical species were taken for the preparation of samples. These boards were stored in a conditioning room at 20 °C and 60 % RH until EMC was reached. The eucalypt samples were obtained from a board stored in green condition (never-dried) at −4 °C and wrapped in polyethylene to prevent moisture loss. The red oak board was selected from a batch of kiln-dried boards conditioned at 20 °C and 40 % RH. All boards were without crook, visible decay, with a minimum of knots and grain distortion. The average basic density (BD, oven dry mass to green volume) of huayruro was 627 kg m^{-3} [coefficient of variation (CV) of 2.4 %], while that of cachimbo, *E. saligna*, and red oak were 569 kg m^{-3} (CV of 2.2 %), 515 kg m^{-3} (CV of 2.6 %), and 490 kg m^{-3} (CV of 1.7 %), respectively.

For MR microimaging studies, small cylinders of 3.6 mm in diameter (transverse to the grain) by 20 mm in length (parallel to the grain) were prepared for each species using a small lathe mounted with a freshly sharpened knife.

Experiments

Three groups of ten matched samples were formed for each species. These groups were destined for three desorption conditions (Table 1). Desorption tests were carried out in a single step procedure from full saturation state for all samples,

Table 1 Characteristics of the moisture sorption conditions used in this experiment (from Goulet and Hernández 1991)

State of sorption	Saturated salt solution	Nominal RH at 21 °C (%)
Desorption	$ZnSO_4$	90
Desorption	NaCl	76
Desorption	NaBr	58

except those of *E. saligna*, whose desorption started from green condition. The re-wetting treatment of samples was done in three steps in order to avoid internal defects in wood structure due to a fast full saturation process (Naderi and Hernández 1997; Almeida and Hernández 2007). The samples were initially placed over a KCl saturated salt solution (86 % RH) for 11 days, followed by 14 days over distilled water (100 % RH). Finally, they were immersed in water and underwent two 24-h cycles of vacuum and atmospheric pressure.

Samples of all groups were then conditioned in desorption over saturated salt solutions inside glass desiccators. These small sorption chambers were placed for long periods in vats filled with water kept at 21 ± 0.01 °C, allowing a precise RH control. A similar procedure has been previously described by Hernández and Bizoň (1994). For each desorption condition, ten samples, one for MR microimaging experiments and nine for EMC assessment, were weighed periodically without being removed from the desiccator until a constant value was reached. The MR microimaging tubes were placed inside the desiccators at the beginning of the sorption test to minimize moisture content (MC) exchange during the tests.

The specimen destined to the MR microimaging experience was placed in the MR microimaging tube (200 mm long, 5 mm outside diameter) once its EMC was reached. A Teflon dowel (180 mm long, 4 mm in diameter) was inserted in the tube to minimize the air space and consequently to reduce MC changes during MR microimaging tests. A tight screw cap sealed the tube. A 25-mm-thick Styrofoam box protected the MR microimaging tubes against any hygrothermal changes during transportation to the University of Montreal, where the MR microimaging tests were done. The tube was weighed before transportation, at the beginning and at the end of the MR microimaging test to detect any MC variation in the sample.

MR microimaging analysis

The MR microimaging tests were done at 21 °C on a 14.1 T Bruker Avance 600 WB spectrometer equipped with a Micro 5 probe, operating at a ^{1}H frequency of 600 MHz. The T_2 relaxation times were calculated by the Carr-Purcell Meiboom-Gill (CPMG) pulse sequence: 90 - [τ -180 - τ]$_n$-acquire. The ^{1}H spectral width was 20 kHz and with an acquisition time of 100 ms. The ^{1}H pulses were applied at field strength of 29 kHz, with a recycle delay of 1 to 2 s.

A standard slice-selective spin-echo imaging sequence was used to acquire images of the ^{1}H present in wood samples. A similar parameter configuration to this

equipment had been used in a previously work (Hernández and Cáceres 2010) for MR microimaging experiments of sugar maple wood. Nevertheless, some adjustments were done in the parameter configuration due to the greater variability and to the heterogeneous characteristics of the four woods studied in this work. A 1-mm-thick slice at the mid-height of each sample was selected by means of sync-shaped selective pulses for all species and sorption conditions. The ^{1}H spectral width was 100 kHz. The selection of a field of view of 4 mm allowed obtaining a nominal in-plane resolution of 40 µm for all images. However, some parameters were adjusted according to each species and sorption condition to obtain the best image quality. These parameters are shown in Table 2. This parameter configuration generated a voxel size of 40 µm of surface and 1 mm of depth, representing an average of multiple and smaller unit data.

Two types of images were acquired from the data contained in the 1-mm slice for all species and sorption conditions. One represents the ^{1}H concentration of the sample, and another represents the distribution of T_2 values. Transverse images were obtained for each of the three desorption conditions and for all species. The images were taken from a section at mid-height of the longitudinal axis of the samples. The digital processing software ParaVision 4.0, Bruker's was used for data acquisition, reconstruction, analysis, and visualization of images. The intensity of ^{1}H concentration images was calibrated according to the images obtained at 90 % RH. However, for T_2 images, this calibration was possible only to red oak wood. A color scale was created to facilitate the visualization, interpretation, and comparison of images. Red represented the highest concentration and black represented no signal in the arbitrary scale for the ^{1}H concentration images. For T_2 images, red indicated a value of T_2 of 6 ms for *E. saligna*, huayruro, and cachimbo. For these species, liquid water is associated with the red, orange, and yellow colors. In the case of red oak, red color indicated a value of 15 ms, being red, orange, yellow, and green an indication of liquid water. There was a gradual transition of colors until a null value of T_2.

Scanning electron microscopy tests

All samples used for MR microimaging scans at 90 % RH were cross-cut using a circular saw at mid-height, i.e., at the same section where the MR microimaging scans were made. The new end-grain section obtained was gingerly refreshed with a sharp microtome blade mounted in a microtome. This was done to match the MR microimages with the scanning electron microscopy (SEM) images. The samples were then oven-dried for 2 h, mounted on standard aluminum stubs with silver paint, and coated with gold/palladium in a sputter coater to obtain transversal images by SEM using a JEOL 840-A microscope.

Table 2 Parameters of MR microimaging used for each species and sorption condition

	Eucalyptus			Huayruro			Cachimbo			Red oak		
	58 %	76 %	90 %	58 %	76 %	90 %	58 %	76 %	90 %	58 %	76 %	90 %
Field strength of ^{1}H pulses (kHz)	12.4	12.4	12.4	12.4	12.4	12.4	25	25	25	25	25	25
Scans	1024	1024	1024	1024	1024	1024	400	400	400	400	400	400
Repetition time (s)	0.6	0.6	0.6	0.6	0.6	0.6	2.0	2.0	2.0	2.0	1.5	1.5
Echo time (ms)	2.5	2.5	2.5	2.5	2.5	2.5	2.3	2.3	2.3	2.3	2.3	2.3
Experience time (min)	340	340	340	340	340	340	1334	1334	1334	1334	1000	1000

Results and discussion

The EMC as a function of RH for the four species studied is given in Fig. 1. The desorption tests were performed from the full-saturated state for huayruro, cachimbo, and red oak hardwoods. Thus, maximum EMCs for each RH were obtained for these species. As a result, the curves in Fig. 1 represent the boundary desorption for these woods. However, for *E. saligna*, the EMC did not correspond to the maximum, given that desorption was conducted in this case from the green state. At 58 % RH, the EMC was slightly higher for *E. saligna* (13.3 %), similar for huayruro (12.4 %) and cachimbo (12.3 %), and slightly lower for red oak (11.8 %). At this RH level, these differences in EMC among species are probably explained by the bound water content variation only. However, as RH increases, the differences in EMC among species become more evident showing, as will be discussed later, an evidence of entrapped liquid water in some species. *Eucalyptus saligna* showed higher sensitivity to changes in RH compared to the other species. This high variation in EMC among species has previously been reported by Almeida et al. (2007) and Hernández (2007b). The difference in EMC observed at 90 % RH could probably have been greater if desorption tests of *E. saligna* had been carried out from the full-saturated state. The low extractive content of *E. saligna* may explain this behavior. Low extractive contents in woods allow a greater availability of sorption sites, which result in higher MC, especially at higher RH (Nzokou and Kamdem 2004; Hernández 2007b).

MR microimaging analysis

As described previously, two types of images were obtained: one showing the ^{1}H concentration distribution and another revealing the T_2 values distribution in the transverse section of the samples. Each voxel of the images represents the average
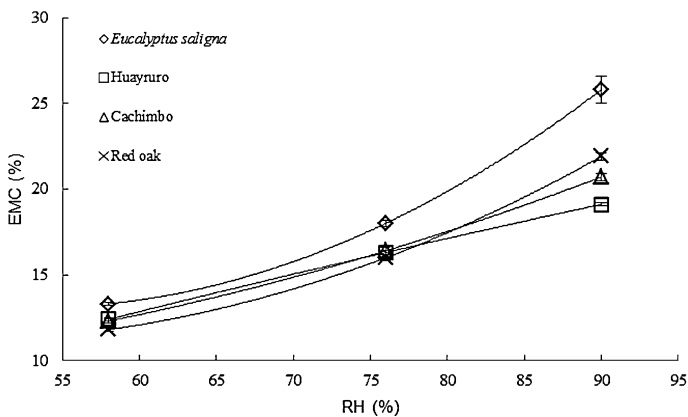

Fig. 1 Equilibrium moisture content (EMC) obtained in desorption as a function of relative humidity (RH) at 21 °C for the four hardwoods studied (standard errors are shown only when it exceeds the *symbol size*)

concentration of ^{1}H or the average T_2 value (1 mm depth). Any element below 40 μm might not be well represented.

Eucalyptus saligna wood

^{1}H concentration and T_2 values of *E. saligna* wood at 90 % RH are represented in Fig. 2a and b, respectively. The images reveal the absence of signal from vessel lumens, indicating that all liquid water has been removed from these elements. Early drainage of vessels has been reported for sugar maple (Hernández and Bizoň 1994; Hernández and Cáceres 2010), and for other hardwoods (Hernández and Pontin 2006; Almeida et al. 2007). Vessels are large tube-like structures responsible mainly for sap transportation. Any free water located in vessel lumens is held by low capillary forces and easily removed, even at high RH.
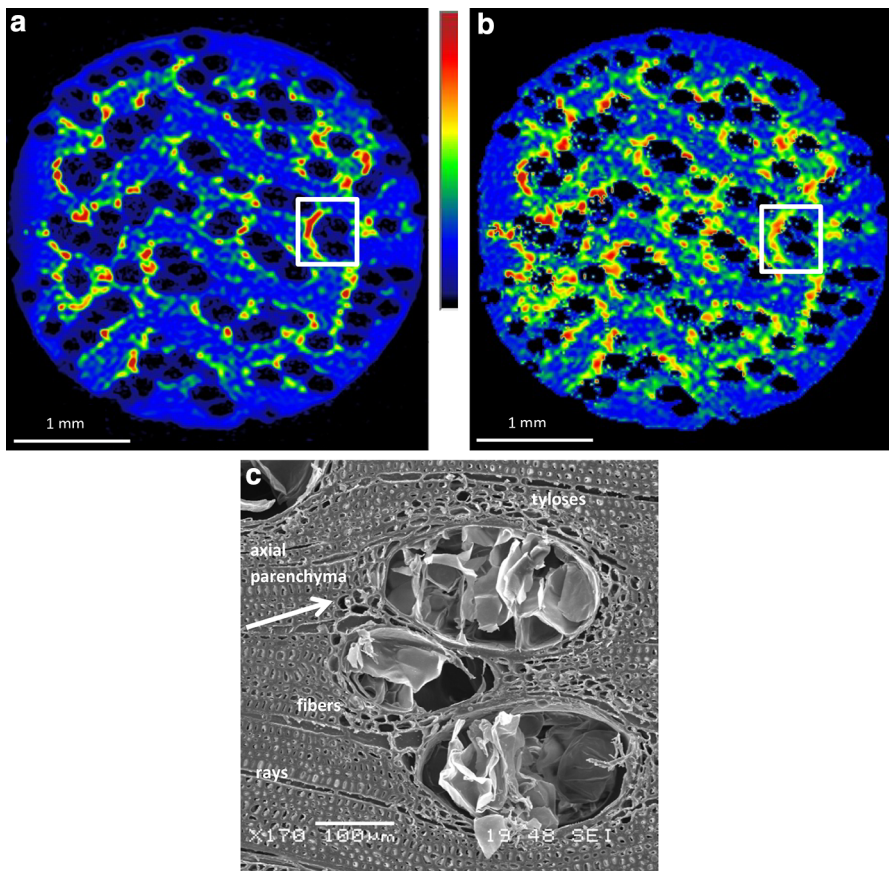

Fig. 2 Transverse MR microimages of *Eucalyptus saligna* samples equilibrated at 90 % RH, representing (**a**) ^{1}H concentration distribution with a global EMC of 25.8 %, and (**b**) corresponding distribution of T_2 values (**c**) SEM image of the section indicated by the *white squares* in (**a**) and (**b**)

The correspondence between high ^{1}H concentration (orange and red spots, Fig. 2a) and T_2 values near 6 ms (orange and red spots, Fig. 2b) indicates that liquid water could be entrapped in *E. saligna* wood structure. This water appears located mainly in areas surrounding the vessels (white squares). These regions correspond to the lumens of the axial parenchyma (Fig. 2c). These tissues have thin-walled cells and generally simple pits. According to Hart et al. (1974), the longitudinal and radial parenchyma are the less permeable flow pathways of water in hardwoods.

The presence of vestured pits connecting axial parenchyma and vessels could provoke the entrapment of liquid water in axial parenchyma lumens. Vestured pits present a pit cavity and/or an aperture wholly or partly lined with projections from the secondary cell wall (IAWA Committee 1989). According to Jansen et al. (2008), these structures could be involved in increasing hydraulic resistance in trees. They were observed in vessel–axial parenchyma pits in some species of the Myrtales order (Jansen et al. 2008), in pits between vessel and ray parenchyma cells of *Eucalyptus regnans* (Scurfield and Silva 1970), in pits of tracheid elements of *Eucalyptus delegatensis* (Singh 1983) and in pit cavities of fiber and vessel walls of *Eucalyptus globulus* and *Eucalyptus camaldulensis* (Watanabe et al. 2006).

Conspicuous tyloses blocking vessels are shown in Fig. 2c. Tyloses are bubble-like outgrowths of the parenchyma cells adjacent to the vessels (Panshin and de Zeeuw 1980). When they are well developed, wood may be difficult to dry or to impregnate with decay-preventive products (Shmulsky and Jones 2011). Therefore, tyloses might constitute another element blocking axial parenchyma–vessel pits, contributing to the entrapment of liquid water in axial parenchyma lumens at 90 % RH.

Therefore, commercial *E. saligna* planks might contain considerable amounts of liquid water blocked in their structure even below FSP. Wood drying of *Eucalyptus* spp. is laborious and at the origin of various defects (Vermaas 1995; Jankowsky and Santos 2005; Jankowsky et al. 2008). This entrapped liquid water might be an additional impediment during drying of *E. saligna*.

Furthermore, the lowest extractive content among the four species considered in this study, as explained previously, and the entrapped liquid water in axial parenchyma cells of *E. saligna*, might explain the highest EMC at 90 %, as illustrated in Fig. 1.

Bound water is represented in Fig. 2a and b by green and blue colors. Green color in Fig. 2a shows a higher concentration of bound water, which appears to be related to the axial parenchyma tissue. Water molecules in this zone could be weakly attached to the sorption sites, as expressed by higher T_2 times (higher molecular motion) (Fig. 2b). On the other hand, blue color shows that bound water is uniformly distributed in fiber and ray cell walls throughout the sample at 90 % RH. Ray cell walls are predominantly uniseriate (97 %) in *E. saligna* (Alzate 2004), with cell walls thinner than the in-plane resolution of the images (40 μm). In this case, it cannot be distinguished between water molecules of fiber and ray walls, justifying therefore the uniformity of the bound water distribution in these two heterogeneous tissues.

The external layers of *E. saligna* sample at 90 % RH (Fig. 2a and b, blue color) reveal that liquid and/or bound water could have been lost during the manipulation

before MR microimaging tests and during the test itself. Likewise, this superficial drying might reflect the easiness of the surface layers of *E. saligna* wood to lose moisture.

The absence of red, orange, and yellow colors at 76 % RH revealed that all liquid water has been drained from *E. saligna* sample (images not shown). Thus, all liquid water has flowed away at some point between 90 % (25.8 % EMC) and 76 % RH (18.0 % EMC). However, *E. saligna* showed a higher EMC than the other species at 76 % RH. In this case, the difference in EMC should be attributed only to bound water. As discussed earlier, the low extractive content in *E. saligna* wood might play a key role in this fact.

Axial parenchyma walls presented slightly higher T_2 values compared to the fiber tissues. Higher T_2 values indicate more molecular motion of water molecules, but these values are low enough to be considered as representing liquid water.

For the 58 % RH condition (13.3 % EMC, images not shown), ^{1}H concentration images represented, as for 76 % RH, uniform ^{1}H concentration throughout the whole section. The blue color was darker, indicating, as expected, lower bound water molecules concentration in the sample at 58 % RH condition. Green color in T_2 images indicates a higher molecular motion in axial parenchyma walls, but without any trace of liquid water.

Huayruro wood

Huayruro wood has a quite heterogeneous anatomy, with a large proportion of axial parenchyma (33.5 %) (Almeida 2006). [1]H concentration and T_2 values of huayruro wood at 90 % RH are represented in Fig. 3a and b, respectively. Contrarily to *E. saligna*, T_2 values of huayruro wood reveal no evidence of entrapped liquid water at 90 % RH, confirming the results of Almeida et al. (2007) for the same species at 90 % RH. However, these authors reported medium T_2 values at 96 % RH (24.8 % EMC), indicating thus the presence of liquid water entrapped in this wood. Therefore, it is highly probable that all liquid water has been drained at some point between 96 % RH (24.8 % EMC) and 90 % RH (19.1 % EMC) (Almeida et al. 2007).

It is worth to note that bound water was not uniformly distributed in huayruro tissues at 90 % RH (Fig. 3a). Blue bands represent axial parenchyma, while yellow, orange, and red spots represent fiber regions crossed by ray tissue. Multiseriate rays are represented by darker blue color in axial parenchyma zone and green color in fiber zone. This clearly reveals the different hygroscopicity of huayruro tissues even under equilibrated MC conditions. Each tissue possesses different EMC under a same water potential, being 19.1 % EMC, an average for the entire sample. A typical SEM image (Fig. 3c) shows that fibers have remarkably thicker cell walls than axial parenchyma and rays. The lumen of fibers is also very small (almost not visible in Fig. 3c), constituting a denser zone in huayruro wood. Parenchyma cell walls are thin-walled and devoid of S2 layer. Thus, axial parenchyma cells and rays have less wood material, and consequently less sorption sites available for water molecules attachment. Moreover, Fig. 3b shows that bound water molecules in fibers have lower T_2 values (blue areas) than in axial parenchyma (blue–green
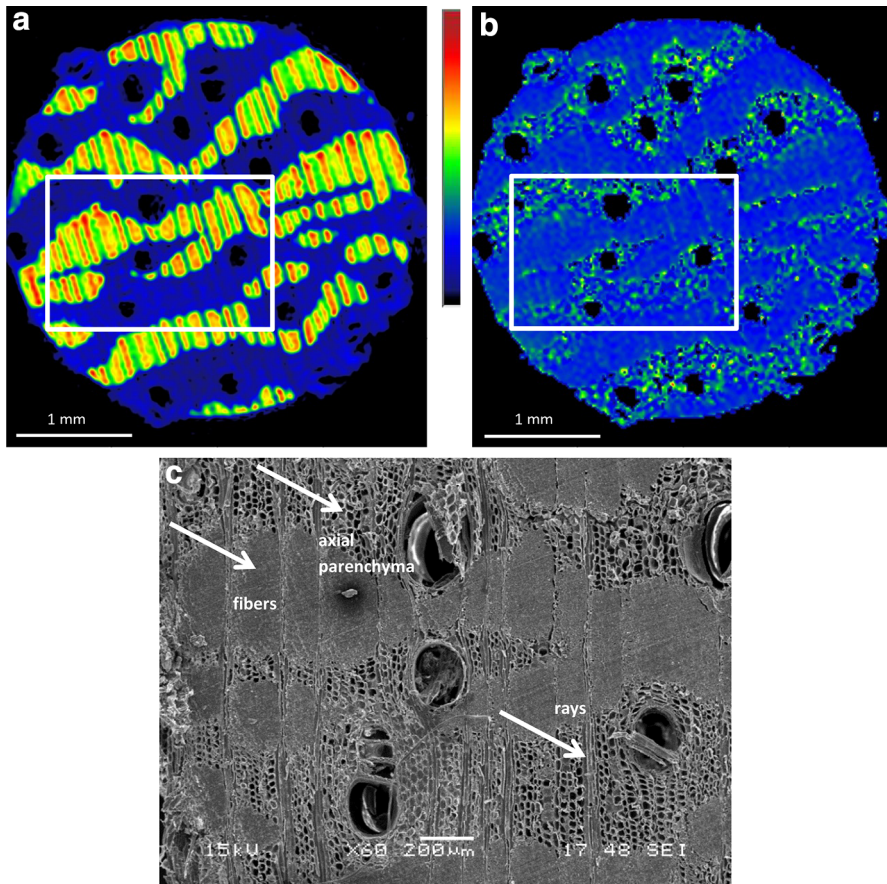
Fig. 3 Transverse MR microimages of huayruro samples equilibrated at 90 % RH, representing (**a**) ^{1}H concentration distribution with a global EMC of 19.1 %, and (**b**) corresponding distribution of T_2 values (**c**) SEM image of the same section indicated by the *white rectangles* in (**a**) and (**b**)

zones), revealing a tighter attachment of water molecules to the sorption sites of fibers. Rays are barely distinguished in Fig. 3b. When visible they constitute green bundles in fiber zone, indicating a higher molecular motion of bound water in their walls than in fiber walls.

As well as at 90 % RH, at 76 % RH, fibers had higher bound water concentration (green, yellow, orange, and red colors) than axial parenchyma (blue zones) and lower T_2 values (image not shown). Multiseriate rays are also represented by darker blue color in axial parenchyma zone and blue color in fiber zone. Therefore, at 76 % RH, the different hygroscopicity of huayruro tissues was still present.

^{1}H concentration images represent, as for 90 and 76 % RH, an inhomogeneous MC distribution for the 58 % RH condition (12.4 % EMC, images not shown). At this RH, moisture content in axial parenchyma and rays was too low to produce a detectable MR signal both for ^{1}H concentration as for T_2 images.

Cachimbo wood

Images of ^{1}H concentration and T_2 values for cachimbo wood at 90 % RH are shown in Fig. 4a and b, respectively. Figure 4b does not show any significant spots representing T_2 values associated with liquid water. Thereby, as for huayruro wood at 90 % RH, no evidence of entrapped liquid water in cachimbo wood was found. As for huayruro wood, bound water was not uniformly distributed in wood tissues even under EMC. In Fig. 4a, red, orange, and yellow colors represent fibers and green color represents rays. Blue and green colors indicate reticulate-apotracheal axial parenchyma and vessels cell walls, respectively. As already discussed for huayruro wood, this heterogeneous moisture distribution under EMC conditions reveals the different hygroscopicity of tissues. In this case, each tissue possesses different MC under a same water potential, being 20.7 % EMC, an average for the entire sample.
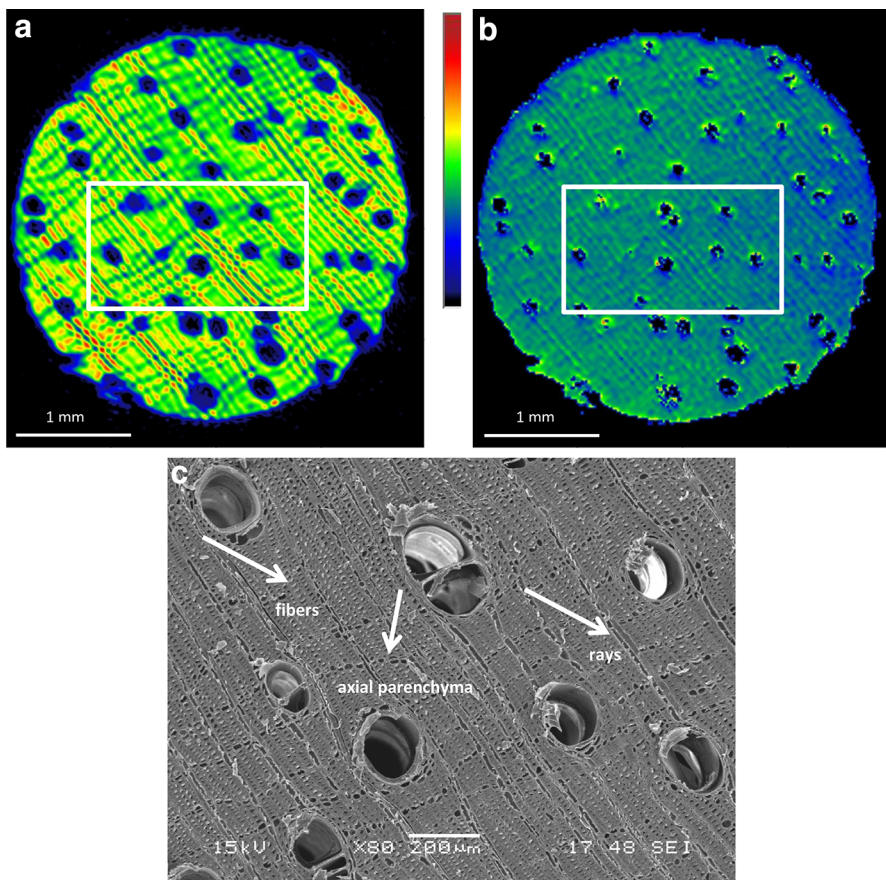

Fig. 4 Transverse MR microimages of cachimbo samples equilibrated at 90 % RH, representing (**a**) ^{1}H concentration distribution with a global EMC of 20.7 %, and (**b**) corresponding distribution of T_2 values (**c**) SEM image of the same section indicated by the *white rectangles* in (**a**) and (**b**)

Rays and axial parenchyma in cachimbo wood may be distinguished from the other elements in Fig. 4b, and they are associated with green color. The same Fig. 4b shows that fibers are represented by blue color. As explained for huayruro, axial parenchyma and ray cells have less wood material and, consequently, less sorption sites available for water molecules attachment, revealing thus higher T_2 times, expressed in Fig. 4b by green color. SEM images (Fig. 4c) reveal in more detail the anatomical structure of cachimbo wood.

At 76 % RH condition, both rays and axial parenchyma showed equivalent ^{1}H concentration (blue color, image not shown). Thus, from 90 to 76 % RH, rays and axial parenchyma lost bound water in a more important rate than fibers (green color, image not shown). Fibers showed a lighter blue color at 58 % RH (image not shown), indicating that they still have higher ^{1}H concentration than rays and axial parenchyma at this RH condition.

Red oak wood

Red oak is a ring-porous wood with very distinct growth rings. Figure 5a and b shows, respectively, MR microimages of ^{1}H concentration and T_2 values of red oak wood at 90 % RH. These images reveal, as for the other three species, the absence of signal from vessel lumens of earlywood and latewood, indicating that all liquid water has been removed from these elements. As discussed for *E. saligna*, early drainage of vessel lumens had been reported for sugar maple (Hernández and Bizoň 1994; Hernández and Cáceres 2010), and for tropical and temperate species (Hernández and Pontin 2006; Almeida et al. 2007; Passarini et al. 2014). The correspondence between high ^{1}H concentration (orange and red spots, Fig. 5a) and T_2 values near 7 ms (green spots, Fig. 5b) indicates that liquid water could be entrapped in the lumen of multiseriate rays and in the lumen of axial parenchyma of latewood (Fig. 5c). According to Siau (1984), earlywood of ring-porous woods is usually much more permeable than that of diffuse-porous woods. Contrarily, uniseriate rays showed no evidence of entrapped liquid water. Red oak wood has very conspicuous multiseriate rays, and narrow uniseriate rays, which are much more numerous (Panshin and de Zeeuw 1980).

According to Côté (1963), uniseriate rays in oak seem to be one of the most permeable elements excluding vessels, and they are clearly more permeable than multiseriate rays. For sycamore wood, low permeability of broad rays may be explained by the lack of pit communication between vessels and rays (Côté 1963). Hart (1984) reported evidence of entrapped liquid water in red oak above 90 % RH, which was located in parenchyma cells. This entrapped liquid water in red oak may explain its higher values of EMC compared to cachimbo and huayruro at 90 % (Fig. 1). At 30 % EMC, Hart (1984) reported that entrapped liquid water could constitute a MC as high as 6–8 % in oak wood.

As for *E. saligna*, the absence of red, orange, yellow color, and significant spots of green color at 76 % RH (images not shown) revealed that all liquid water has been drained from red oak. Thus, the drainage of all liquid water was accomplished at some point between 90 % (21.9 % EMC) and 76 % RH (16.0 % EMC). Bound water was uniformly distributed in red oak samples at this RH level.
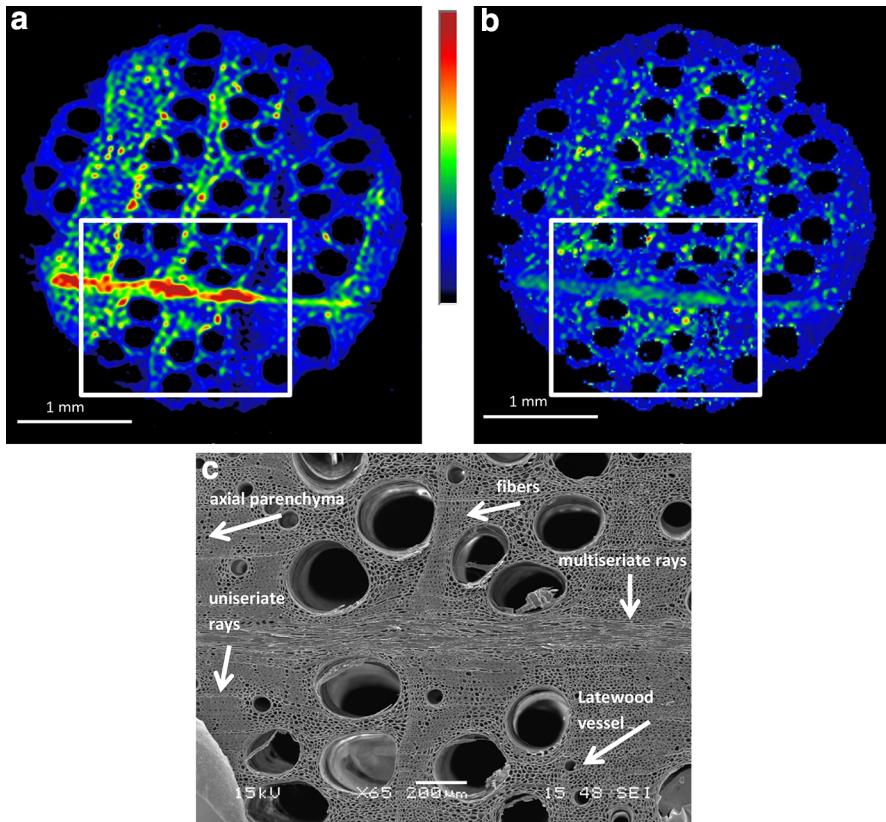
Fig. 5 Transverse MR microimages of red oak samples equilibrated at 90 % RH, representing (**a**) ^{1}H concentration distribution with a global EMC of 21.9 %, and (**b**) corresponding distribution of T_2 values (**c**) SEM image of the same section indicated by the *white rectangles* in (**a**) and (**b**)

For the 58 % RH condition (11.8 % EMC, images not shown), ^{1}H concentration images represent, as for 76 % RH, uniform ^{1}H concentration throughout the whole section. However, the blue color is darker, indicating, as expected, lower bound water molecules concentration in the sample at 58 % RH condition.

Conclusion

The liquid and bound water distributions in wood samples under three EMCs below FSP were studied by MR microimaging techniques. Desorption experiments were carried out at 21 °C from full-saturated state and from green condition on four hardwood species. The main conclusions are listed below:

1. MR microimages based on ^{1}H concentration coupled with T_2 values distribution images are a useful nondestructive tool for mapping MC distribution on

heterogeneous hardwoods, contributing to a better understanding of wood–water relations.

2. MR microimaging confirms that liquid water may be found entrapped in wood structure below FSP under equilibrated conditions, even in small samples. In this case, wood lost bound water in the presence of liquid water, contradicting the concept of FSP.

3. Parenchyma cells (axial parenchyma and rays) seem to be a reservoir of entrapped liquid water below FSP in difficult to dry and collapse prone species, as *E. saligna* and red oak. Occluded pits and/or poor communication between parenchyma and vessels might explain this fact.

4. For huayruro and cachimbo wood, even at a global EMC, the images showed that bound water was not uniformly distributed in wood structure, concentrating more in fibers than parenchyma for both species. Therefore, moisture concentration varied according to the wood tissue, revealing that denser tissues are more hygroscopic than lighter ones.

References

Almeida G (2006) Influence de la structure du bois sur ses propriétés physico-mécaniques à des teneurs en humidité élevées. (Influence of the wood structure on its physical and mechanical properties at high relative humidities). Ph.D. thesis, Université Laval, Québec, Canada **(in French)**

Almeida G, Hernández RE (2006a) Changes in physical properties of tropical and temperate hardwoods below and above the fiber saturation point. Wood Sci Technol 40:599–613

Almeida G, Hernández RE (2006b) Changes in physical properties of yellow birch below and above the fiber saturation point. Wood Fiber Sci 38:74–83

Almeida G, Hernández RE (2007) Dimensional changes of beech wood resulting from three different re-wetting treatments. Holz als Roh-und Werkstoff 65:193–196

Almeida G, Gagné S, Hernández RE (2007) A NMR study of water distribution in hardwoods at several equilibrium moisture contents. Wood Sci Technol 41:293–307

Almeida G, Leclerc S, Perré P (2008) NMR imaging of fluid pathways during drainage of softwood in a pressure membrane chamber. Int J Multiph Flow 34:312–321

Alzate SBA (2004) Caracterização da madeira de árvores de clones de *Eucalyptus grandis*, *E. saligna* e *E. grandis* x *urophylla*. (Wood characterization of *Eucalyptus grandis*, *E. saligna*, and *E. grandis* x urophylla clones). Ph.D. thesis, Universidade de São Paulo, Piracicaba, Brazil **(in Portuguese)**

Araujo CD, MacKay AL, Hailey JRT, Whittall KP, Le H (1992) Proton magnetic resonance techniques for characterization of water in wood: application to white spruce. Wood Sci Technol 26:101–113

Araujo CD, MacKay AL, Whittall KP, Hailey JRT (1993) A diffusion model for spin–spin relaxation of compartmentalized water in wood. J Magn Reson B 101:248–261

Babiak M, Kúdela J (1995) A contribution to the definition of the fiber saturation point. Wood Sci Technol 29:217–226

Barkas WW (1935) Fibre saturation point of wood. Nature 135:545

Brownstein KR (1980) Diffusion as an explanation of observed NMR behavior of water absorbed on wood. J Magn Reson 40:505–510

Brownstein KR, Tarr CE (1979) Importance of classical diffusion in NMR studies of water in biological cells. Phys Rev A 19:2446–2453

Bucur V (2003) Techniques for high resolution imaging of wood structure: a review. Meas Sci Technol 14:R91–R98

Côté WA (1963) Structural factors affecting the permeability of wood. J Polym Sci C 2:231–242

Dvinskikh SV, Henriksson M, Berglund LA, Furo I (2011) A multinuclear magnetic resonance imaging (MRI) study of wood with adsorbed water: estimating bound water concentration and local wood density. Holzforschung 65:103–107

Goulet M, Hernández RE (1991) Influence of moisture sorption on the strength of sugar maple wood in tangential tension. Wood Fiber Sci 23:197–206

Hameury S, Sterley M (2006) Magnetic resonance imaging of moisture distribution in *Pinus sylvestris* L. exposed to daily indoor relative humidity fluctuations. Wood Mater Sci Eng 1:116–126

Hart CA (1984) Relative humidity, EMC, and collapse shrinkage in wood. For Prod J 34(11/12):45–54

Hart CA, Przestrzelski PJ, Wheeler FJ (1974) Entrapped lumen water in hickory during desorption. Wood Sci 6:356–362

Hernández RE (2007a) Effects of extraneous substances, wood density and interlocked grain on fiber saturation point of hardwoods. Wood Mater Sci Eng 2:45–53

Hernández RE (2007b) Moisture sorption properties of hardwoods as affected by extraneous substances, wood density, and interlocked grain. Wood Fiber Sci 39:132–145

Hernández RE, Bizoň M (1994) Changes in shrinkage and tangential compression strength of sugar maple below and above the fiber saturation point. Wood Fiber Sci 26:360–369

Hernández RE, Cáceres CB (2010) Magnetic resonance microimaging of liquid water distribution in sugar maple wood below fiber saturation point. Wood Fiber Sci 42:259–272

Hernández RE, Pontin M (2006) Shrinkage of three tropical hardwoods below and above the fiber saturation point. Wood Fiber Sci 38:474–483

Hoffmeyer P, Engelund ET, Thygesen LG (2011) Equilibrium moisture content (EMC) in Norway spruce during the first and second desorptions. Holzforschung 65:875–882

Hsi E, Hossfeld R, Bryant RG (1977) Nuclear magnetic resonance relaxation study of water absorbed on milled Northern white cedar. J Colloid Interface Sci 62:389–395

IAWA Committee (1989) IAWA list of microscopic features for heartwood identification. Int Assoc Wood Anat Bull 10:219–332

Jankowsky IP, Santos GRV (2005) Drying behaviour and permeability of *Eucalyptus grandis* lumber. Maderas. Ciencia y tecnología 7(1):17–21

Jankowsky IP, Santos GRV, Andrade A (2008) Secagem da madeira serrada de eucalipto (Drying behavior of eucalyptus lumber). Revista da Madeira 19:64–72 **(In Portuguese)**

Jansen S, Pletsers A, Rabaey D, Lens F (2008) Vestured pits: a diagnostic character in the secondary xylem of myrtales. J Trop For Sci 20:328–339

Kastler B (2011) Comprendre l'IRM: Manuel d'autoapprentissage (Understanding MRI: self-study manual), Masson, Paris, 2011 **(in French)**

Meder R, Codd SL, Franich RA, Callaghan PT, Pope JM (2003) Observation of anisotropic water movement in *Pinus radiata* D. Don sapwood above fiber saturation using magnetic resonance micro-imaging. Holz als Roh-und Werkstoff 61:251–256

Menon RS, MacKay AL, Hailey JRT, Bloom M, Burgess AE, Swanson JS (1987) An NMR determination of the physiological water distribution in wood during drying. J Appl Polym Sci 33:1141–1155

Naderi N, Hernández RE (1997) Effect of a re-wetting treatment on the dimensional changes of sugar maple wood. Wood Fiber Sci 29:340–344

Navi P, Heger F (2005) Comportement thermo-hydromécanique du bois (Thermo-hydro-mechanical behavior of wood), Presses Polytechniques et Universitaires Romandes, Switzerland **(in French)**

Nzokou P, Kamdem DP (2004) Influence of wood extractives on moisture sorption and wettability of red oak (*Quercus rubra*), black cherry (*Prunus serotina*), and red pine (*Pinus resinosa*). Wood Fiber Sci 36:483–492

Panshin AJ, de Zeeuw C (1980) Textbook of wood technology. Michigan State University, New York

Passarini L, Malveau C, Hernández RE (2014) Water state study of wood structure of four hardwoods below fiber saturation point with NMR technique. Wood Fiber Sci 46:480–488

Quick JJ, Hailey JRT, Mackay AL (1990) Radial moisture profiles of cedar sapwood during drying—a proton magnetic-resonance study. Wood Fiber Sci 22:404–412

Ross RJ, Brashaw BK, Pellerin RF (1998) Nondestructive evaluation of wood. Forest Prod J 48:14–19

Scurfield G, Silva SR (1970) The vestured pits of *Eucalyptus regnans* F.Muell.: a study using scanning electron microscopy. Bot J Linn Soc 63:313–320

Shmulsky R, Jones P (2011) Forest products and wood science, an introduction. Blackwell, Ames

Siau JF (1984) Transport processes in wood. Springer, Berlin

Siau JF (1995) Wood: influence of moisture on physical properties. Virginia Tech, Blacksburg

Singh AP (1983) On the occurrence of anomalous tubular structures in the vestured pits of petiolar xylem in *Eucalyptus delegatensis*. IAWA Bull 4:239–243

Skaar C (1988) Wood–water relations. Springer, Berlin

Stamm AJ (1964) Wood and cellulose science. Ronald Press, New York

Stamm AJ (1971) Review of nine methods for determining the fiber saturation point of wood and wood products. Wood Sci 4:114–128

Stone JE, Scallan AM (1967) The effect of component removal upon the porous structure of the cell wall of wood II. Swelling in water and the fiber saturation point. Tappi 50:496–501

Telkki V-V (2012) Wood characterization by NMR & MRI of fluids. eMagRes 1:215–222

Thygesen LG, Elder T (2008) Moisture in untreated, acetylated, and furfurylated Norway spruce studied during drying using time domain NMR. Wood Fiber Sci 40:309–320

Tiemann HD (1906) Effect of moisture upon the strength and stiffness of wood. USDA For Serv, Bull 70, Government Printing Office, Washington, DC

Vermaas HF (1995) Drying eucalyptus for quality: material characteristics, pre-drying treatments, drying methods, schedules and optimisation of drying quality, South African. For J 174:41–49

Watanabe Y, Sano Y, Asada T, Funada R (2006) Histochemical study of the chemical composition of vestured pits in two species of Eucalyptus. IAWA J 27:33–43